Analysis of multi-temporal image series for the preventive conservation of varnished wooden surfaces

Alireza Rezaei[1][0000−0001−5067−2030], Sylvie
Le Hégarat-Mascle[1][0000−0001−8494−2289], Emanuel Aldea[1][0000−0001−7065−4809],
Piercarlo Dondi[2,4][0000−0002−0624−073X], and Marco
Malagodi[3,4][0000−0003−4286−6331]

[1] SATIE Laboratory, University Paris Saclay, rue Noetzlin, Gif-sur-Yvette 91190, France
firstname.lastname@universite-paris-saclay.fr
[2] Department of Electrical, Computer and Biomedical Engineering, University of Pavia,
Via Ferrata 5, 27100, Pavia, Italy piercarlo.dondi@unipv.it
[3] Department of Musicology and Cultural Heritage, University of Pavia,
Corso Garibaldi 178, 26100, Cremona, Italy marco.malagodi@unipv.it
[4] CISRiC - Arvedi Laboratory of Non-Invasive Diagnostics, University of Pavia,
Via Bell'Aspa 3, 26100, Cremona, Italy

Abstract. Preventive conservation is a vital practice in Cultural Heritage that consists in the constant monitoring of the state of conservation of an artwork, with the final goal of minimizing the risk of damages and thus, to reduce the need of restorations. In this work, we propose a probabilistic approach for analyzing alterations appearing on varnished wooden surfaces (such as those of historical violins) based on an a-contrario framework. Our method works on time series of images, it is robust to noise and avoids parameter tuning as well as any assumption about the quantity and the shape of the worn-out areas. Furthermore, the proposed algorithm is adapted to the context of preventive conservation, with few data samples and imprecise annotations. As test set, we used image sequences included in the "Violins UVIFL imagery" dataset. Results illustrate the capability of the proposed method to distinguish altered areas from the surrounding noise and artifacts.

Keywords: A-contrario methods · Cultural heritage · Preventive conservation

1 Introduction

In the Cultural Heritage field, preventive conservation, namely the constant monitoring of the state of conservation of artworks and monuments, is becoming a common practice, fundamental to reducing the risk of damages and the need of restorations [4,28]. Handling an effective preventive conservation is particularly complex and, generally, requires an interdisciplinary approach to properly interpret and manage the effects of chemical, physical, and biological alterations [19,33,34]. In this context, image processing can be helpful to simplify the overall procedure. Even if images alone are not enough to perfectly characterize the state of an artwork, they are ideal to provide a quick preliminary examination and to identify regions of interest on a surface. This paper addresses this specific problem, focusing in particular on varnished wooden surfaces.

The varnishes applied on wooden surfaces of historical relics are generally delicate and can be easily damaged if the artifact is not properly handled. Historical musical instruments, such as violins or violas, are a common example of artworks with a varnished wooden surface that can be subject to wear. In fact, differently from other artworks that are simply held in museums, historical musical instruments are occasionally played even today, leading to a clear risk of mechanical wear, especially in those areas in direct contact with the musician.

Varnished wooden surfaces present various complexities: firstly, they are generally highly reflective, thus, noisy reflections, that can be confused for alterations, are common during photo acquisition; secondly, varnish wear can evolve in different ways depending on both the initial conditions of the surface and the different substances present; finally, the surface can be very complex and stratified due to multiple restorations occurred during centuries (which is very common for historical violins).

The combined use of multiple analytical techniques has proved beneficial for handling these issues [15,40], however, as previously said, this "traditional" preventive conservation approach is very time consuming. A more efficient procedure should consist of regular but rapid optical analysis of the images to quickly identify *possible* altered areas. The result of this analysis will indicate where a more thorough multi-modal analysis is needed. Image acquisition is very fast compared to other chemical-physical examinations, thus, ideally, using image processing, it would be possible to frequently examine the state of conservation of one or more artworks in a limited amount of time.

In this work, we describe a probabilistic method for early detection and analysis of alterations through a multi-temporal image series. We specifically work with varnished wooden surfaces subjected to mechanical wear over time. Our proposition is based on the a-contrario framework [10,9] and it improves the method presented in [37] which deals with detection of changes between two single frames: a reference image and an up-to-date acquisition. In this study, we extend the detection framework in order to process a temporal sequence of changes and to account thus for their significance with respect to the spatial plus time dimensions. The main novelty of our work is that the analysis is focused on the evolution of the alterations in time, which in turn allows us to detect the wear earlier and more reliably. This way, we can successfully handle noise and artifacts that would have been detrimental in change detection between only two frames.

The remainder of the paper is structured as follows: Section 2 provides a brief overview of the state of art; Section 3 discusses the proposed approach; Section 4 discusses the experiments; and finally, Section 5 draws the conclusions.

2   Related Works

2.1   Change and damage detection

In recent years, change detection has been tackled with deep neural networks for a variety of applications, among which remote sensing, traffic and medical monitoring, or quality control in manufacturing [43,24,29,25,42,46]. Typically, the feature extraction modules of these architectures are fine-tuned on an appropriate quantity of samples

of the target domain in order to reach high levels of task accuracy. In our considered application however, the relative scarcity of the data coupled with the high level of imprecision of the expert annotations favor statistical approaches in which prior information may be more readily integrated into the models. This is a common problem in the Cultural Heritage field. Even if machine and deep learning approaches are used, their adoption is not widespread as in other fields, mainly due to the limited availability of data [16].

In Cultural Heritage, methods for automatic wear and damage detection mainly rely on traditional computer vision techniques, but nevertheless they proved to be very useful and applicable in different scenarios. A widely studied topic is the detection of crack in paintings. Notable approaches in this field include the use of content-based analysis [1], the extension of morphological operations to hyper-spectral images [8] and the combination of elongated filters, multiscale morphology and K-SVD [7], subsequently improved using multimodal data [35].

Another related topic is the damage detection in stone artifacts. For example, Gelli et al. [18] used Shape from Shading for identifying degradation in historical buildings; Cerimele and Cossu [5] identified decay in ancient monuments using fast marching numerical method; while Manfredini et al. [30] used a combination of 2D and 3D segmentation to discriminate among different types of deterioration.

Image processing techniques are also used for monitoring the decay of frescoes [21] and even for detecting damaged archaeological sites from space [6].

Despite their wide applicability, computer vision methods are still rarely used for wear detection in varnished wooden surfaces, as those of historical musical instruments. Attempts have been made to detect areas with established wear, that had peculiar chromatic characteristics [13]. More recently, Rezaei et al. [36,37] proposed a method for detecting changed pixels between two multi-modal images and then grouping them together, while Dondi et al. [14] presented a segmentation approach based on histogram quantization and genetic algorithm. However, all these works study the evolution of alterations using no more than two frames at a time.

2.2   A-contrario framework

Since wear areas are highly variable, we look for some approaches which can handle the difficulties in wear detection (unknown shape, unknown distribution, high amount of noise) and at the same time can give us a criterion to judge how *surprising* a certain arrangement of points is. Both spatially and temporally extraordinary closeness of points could indicate a wear region. The a-contrario framework introduced by Desolneux et al. [10] has the potential to satisfy the mentioned requirements. Across the computer vision field, it has been used in variety of areas such as texture analysis [20], motion detection [44,45], edge and line detection [47,2,3], or reconstruction from motion [32]. At the same time, grouping principles have been used for tasks related to the higher-level perceptual organization of scenes as well [31,48], owing to their general nature.

In our case, we are interested in the applications dealing with the detection of changed areas across multi-temporal images. In early studies, Lisani and Morel [26] used a-contrario framework and spectral invariant features to detect meaningful changes

between two satellite images of the same area taken in different times. In 2007, Rousseau et al. [39] proposed an a-contrario approach for change detection in three dimensional multi-modal medical images such as Magnetic Resonance sequences. In 2010, a similar approach was proposed by Robin et al. [38] for sub-pixel change detection in a time-series of satellite images. Flenner and Hewer [17] further investigated this approach by using exchangeable random variables instead of independent and identically distributed (IID) assumption. As a later example, Liu et al. [27] applied a-contrario framework for comparing very high-resolution images of urban areas.

In the field of preventive conservation, a-contrario framework has been used for comparison of two single images to detect candidate points (seed detection) and then group them together (clustering) [36]. Later, Rezaei et al. [37] introduced a noise model to detect in one step very unlikely (under noise model assumption) arrangements of pixels based both on their location and their gray-level value. They assume the gray-level values to be a third axis and introduce a custom 3D distance to relate all three axes together. While this approach handles some of the aforementioned problems; it still only works with two frames of the series at a time, missing some potentially very useful information present in the evolution of the clusters through time to make the distinction between wear and noise more evident. The current paper aims to introduce to notion of time into the a-contrario framework through the definition of the noise model and the computation of the number of false alarms.

3   Proposed approach

Let $\{I_t\}_{t=0}^{n}$ be a series of n multi-temporal RGB images taken from a varnished wooden sample; I_0 being the reference image. The size of each I_t is $w \times h$. We perform the change detection in each $I_t(t > 0)$ image with respect to I_0 using the method described in [37]. This results in a set of binary images denoted $\{B_t\}_{t=1}^{n}$. It is important to note that this step is not part of the algorithm; therefore, it can be performed using any proper 2D change detection and clustering algorithm. If the 2D change detection method outputs a change map, it needs to be converted to a binary image prior to being used in the following steps. The proposed algorithm gets this series of binary images as input.

The following sections summarize each step of the algorithm that produces as output, three dimensional clusters ranked based on their significance.

3.1   Distance matrix

Considering the whole series $\{B_t\}_{t=1}^{n}$, we create the $3D$ point cloud $\mathcal{P}$ with the two spatial lines and columns axes of each image alongside time as the third axis (Fig. 1):

$$\mathcal{P} = \{(x, y, z), x \in \{1, 2, \ldots, w\}, y \in \{1, 2, \ldots, h\}, z|z/c_t \in \{1, 2, \ldots, n\}\}, \quad (1)$$

where c_t is the time coefficient; a real valued constant that controls the importance of a distance in time compared to a distance in image space. If $c_t = 1$, then we give the same importance to both.
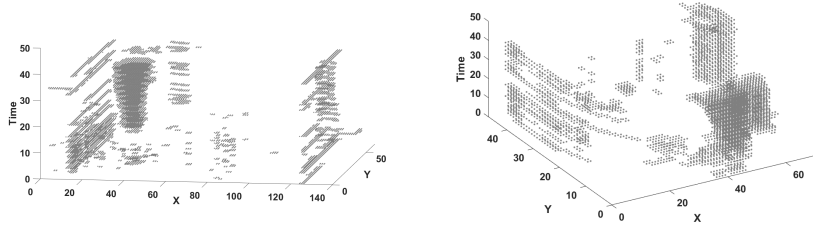
Fig. 1: Point cloud $\mathcal{P}$ derived from the sequence WS01 (left) and SV01 (right). X and Y axes are in pixels, while the time dimension (Z axis) depends on the factor c_t (in these experiments $c_t = 2$).

After constructing $\mathcal{P}$, we aim to segment it into 3D clusters and rank them based on their visual significance in the 3D (2D + time) space. The cluster detection using the a-contrario approach is based on point distance [11]. A Euclidean distance between the points of $\mathcal{P}$ automatically considers their spatial proximity as well as their closeness in time. The distance matrix D is constructed by computing the 3D distance between each pair $(x_a, y_a, z_a), (x_b, y_b, z_b) \in \mathcal{P}$:

$$D_{a,b} = \sqrt{(x_a - x_b)^2 + (y_a - y_b)^2 + (z_a - z_b)^2}. \tag{2}$$

3.2 Number of False Alarms

In order to define and evaluate the significance of the clusters formed by any subset of points in $\mathcal{P}$, we use an a-contrario criterion. Our naive model $\mathcal{M}$ represents spatial and temporal inconsistency for the points in $\mathcal{P}$. Specifically,

Definition 1 (Naive model $\mathcal{M}$) *The set of points $\mathcal{P}$ is a random set of $|\mathcal{P}|$ independent uniformly distributed variables over the 3D cube of the image series ($[1, w] \times [1, h] \times [1, n \times c_t]$).*

Let us consider a sub-volume O in the image cube; the probability that a point belongs to O, under the naive model $\mathcal{M}$, is given as:

$$p_O = \frac{V_O}{w \times h \times n \times c_t}, \tag{3}$$

where V_O is the volume of O. The probability $\mathbb{P}_{\mathcal{M}}(p_O, |\mathcal{P}|, \kappa)$ of observing κ points within O by chance, is given by the tail of the binomial distribution. The Number of False Alarms (NFA) can then be derived by extending the formulation proposed in [9] to 3D clusters:

$$NFA(p_O, |\mathcal{P}|, \kappa) = N_{test} \times \sum_{i=\kappa}^{|\mathcal{P}|} \binom{|\mathcal{P}|}{i} p_O^i (1 - p_O)^{|\mathcal{P}|-i}. \tag{4}$$

In practice, the volume V_O needed for the computation of the term p_O^i, is estimated as the *lower bound* of the volume of the points in O which can form any 3D shape. The term $(1 - p_O)$ on the other hand represents the relative volume of the region that is definitely outside the cluster i.e., outside the *upper bound* of the cluster. These two volumes are calculated by morphological operations extending the approach detailed in [9] to work with 3D data. It is worth noting that the distance between each two points indicated in D is defined as a 3D Euclidean distance; therefore, the morphological operations used here are usual dilation and erosion with a 3D kernel.

In Eq. (4), N_{test}, called the numbers of tests, controls the average number of false alarms [11]. In this work, we make this number constant for a given image cube (image series), i.e., independent of the considered cluster O, so that it is not involved in NFA minimization.

3.3   Maximal clusters

Using Eq. (2) a minimum spanning tree is created for the points in $\mathcal{P}$. Using this tree, we group the points from smallest cluster(s) (nearest couple of points) to the biggest cluster (all points). For each cluster, we compute the NFA using Eq. (4). The used ranking criterion for clusters (O containing κ points) is their meaningfulness $\mathcal{S}$ defined as:

$$\mathcal{S}(O) = -\log(NFA(p_O, |\mathcal{P}|, \kappa)). \tag{5}$$

In our case, we want to partition $\mathcal{P}$; therefore, from all the possible clusters of points in $\mathcal{P}$, only the *maximal* clusters are considered, with *maximal* clusters defined according to [9]:

Definition 2 *A cluster $\mathcal{C} \subset \mathcal{P}$ is said maximal if $\forall \mathcal{L} \subsetneq \mathcal{C}, \mathcal{S}(\mathcal{L}) < \mathcal{S}(\mathcal{C})$ and $\forall \mathcal{L} \supsetneq \mathcal{C}, \mathcal{S}(\mathcal{L}) \leq \mathcal{S}(\mathcal{C})$.*

The list of maximal clusters sorted by their $\mathcal{S}$ value is the output of the algorithm. The cluster with the highest $\mathcal{S}$ is most significant cluster in the image series.

4   Experiments

4.1   Dataset

As test set, we used the "Violins UVIFL imagery" dataset[5] [14], a collection of multi-temporal UV induced fluorescence (UVF or UVIFL) images, referring to both real instruments and artificially altered samples created in laboratory.

UVIFL photography is a well-known non-invasive diagnostic technique that allows us to observe details not perceivable using visible light [23]. For example, in the case of historical violins, UVIFL images are commonly used to highlight possible restorations or regions of interest where it would be advisable to apply more precise but slower diagnostic techniques [12], such as X-Ray Fluorescence (XRF) [41] or Fourier Transform Infrared (FTIR) spectroscopy [22]. The capability to see "hidden" details of a surface is

---

[5] https://vision.unipv.it/research/UVIFL-Dataset/

particularly valuable for our goal since it potentially allows for an early detection of new alterations. Please note that UV induced fluoresce is a phenomenon due to the specific properties of substances commonly used in the varnishes, that react to the light in the UV-A spectrum (315 - 400 nm) re-emitting radiations in the visible spectrum (400-700 nm), and thus, the image acquisition is performed with a standard RGB camera [12].

In our experiments we focused only on the artificially created sequences present in the dataset, since those referring to real historical violins contain only three sessions each, too few for performing a proper multi-temporal analysis. Each sequence consists in one to three images of the initial state of the sample and then a series of subsequent frames where the surface was altered, and the wear starts and grows. We use the following sequences from the dataset: WS01, a 20-frame sequence that displays the appearing and the growing of an alteration in an area with intact varnish; and SVO1, a 20-frame sequence that shows the growing of an already worn-out region on a sample violin back plate.

4.2 Results

Using the sequences WS01 and SV01, for each frame, we generate binary change images respect to the reference frame, applying the method described in [37]. Figures 2 and 3 show, respectively for WS01 and SV01, four sample frames and their corresponding binary image.
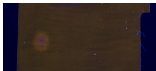
No.	UVIFL image	Input binary image	Detection results	Ground truth
10				
14				
16				
20				

Fig. 2: Four sample frames from the sequence WS01 and their corresponding cluster detection results. At each frame, the first, second and third cluster according to decreasing order of meaningfulness are shown in red, green, and blue, respectively.
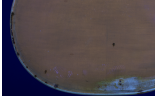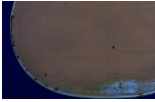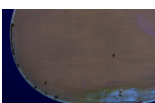
No.	UVIFL image	Input binary image	Detection results	Ground truth
8				
12				
16				
20				

Fig. 3: Four sample frames from the sequence SV01 and their corresponding cluster detection results. At each frame, the first, second and third cluster according to decreasing order of meaningfulness are shown in red, green, and blue, respectively.

Figure 1 shows the point cloud created by accumulating the change detection results for each frame of both sequences. The coefficient c_t is set to 2 (this gives slightly more importance to spatial proximity over time proximity, penalizes the clusters which disappear in some frames and keeps the size of the representation domain small enough for a better performance). The time domain is the upward axis in all visualizations. As we can see, there is a considerable amount of noise present in both point clouds. In addition, there are two sets of artifacts in the left and right sides of both sequences, which are related to the UV reflections from the the wooden sample.

In practice, the optical monitoring of a varnished wooden surface is an ongoing and never-ending process. This means that the number of available frames and the accuracy of the detection increases as the time goes on. Of course, if the sequence of available images becomes too large, we only keep the last n frames with n chosen as a compromise between computation resources and detection performance. In our case, we keep every frame available from the first until the last one.

To simulate a practical optical monitoring process and to analyze different detection results in any given point in time, we started the experiment with 10 frames for the sequence WS01 and 8 for the sequence SV01; then, we ran the algorithm repeatedly

(a) $t \in [1, 10]$ (b) $t \in [1, 14]$ (c) $t \in [1, 16]$ (d) $t \in [1, 20]$
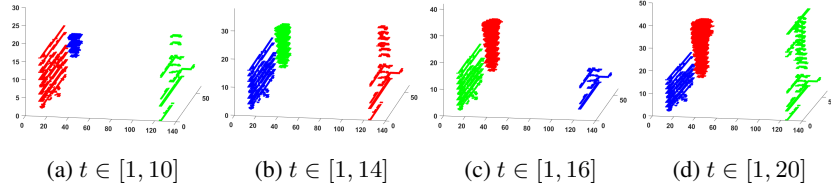
Fig. 4: Evolution of the detection by increasing the number of used time frames t in the sequence WS01. Color code gives the rank according to significance: red first, green second, blue third. The time domain is the upward axis in all visualizations.

(a) $t \in [1, 8]$ (b) $t \in [1, 12]$ (c) $t \in [1, 16]$ (d) $t \in [1, 20]$
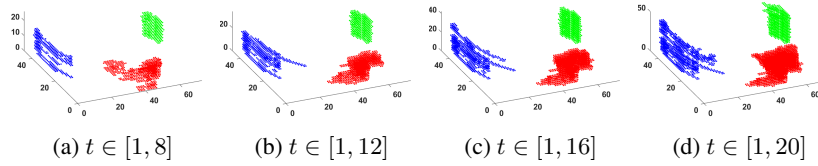
Fig. 5: Evolution of the detection by increasing the number of used time frames t in the sequence SV01. Same conventions of Fig. 4.
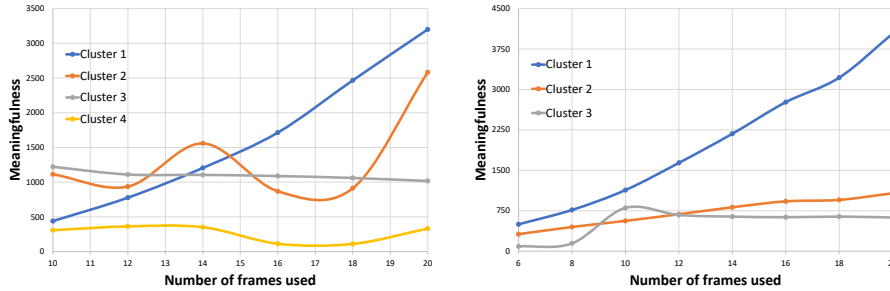
Fig. 6: The evolution of the meaningfulness value of sample clusters in different runs of the algorithm for sequence WS01 (left) and SV01 (right).

increasing the considered number of frames in each run until processing all frames. Each run gives us a list of clusters sorted by their meaningfulness value. The rank of each cluster among the whole set of clusters can change from one run to another. In general, assuming that the wear region expands over time, our expectation is that the wear starts in lower ranks and steadily rises to the first rank. We can also follow the evolution of the meaningfulness value from one run to the next. Again, we expect that the significance of the wear region increases as we get more frames. On the other hand, the meaningfulness value for the noise and artifact clusters should remain nearly unchanged or go up and down randomly. Another difference between the wear region and the rest is that it shall be present in every frame after its first appearance. Therefore,
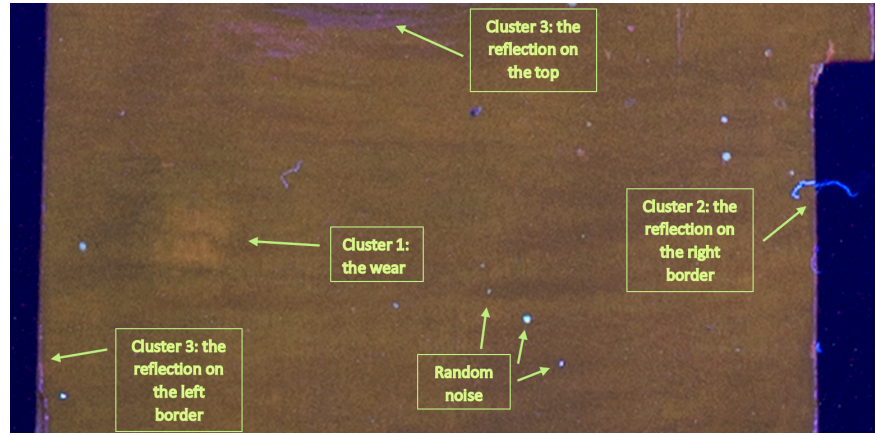
Fig. 7: Location of clusters 1 to 4 on a sample frame (frame 8) from the sequence WS01.

it is possible that a detected area is divided into two clusters along the time axis. In that case, we only take into account the one with the highest meaningfulness.

Figures 4 and 5 illustrate the detection results through time, i.e., based on the number of frames used as input. In each case, the top three clusters have been shown. As one may notice, firstly, only clusters which are consistent have been detected. Minor artifacts and small noises have been disregarded, a fact which is a very desirable behavior when multi-temporal information is available. Secondly, the region of interest which is the actual changed area has been chosen by the end of the sequence as the most significant cluster. The evolution of meaningfulness of each cluster for the two sequences is depicted in Fig. 6.

For a more in-depth analysis, we can consider the four main clusters present in the sequence WS01 (see Fig. 7 for their location on a sample frame) and as a result in $\mathcal{P}$:

– Cluster 1: the wear area.
– Cluster 2: the artifact related to the right border.
– Cluster 3: the artifact related to the left border.
– Cluster 4: the noise present in the upper part of some frames.

Considering the left chart in Fig. 6, which illustrates the meaningfulness values for these four clusters in each run of the algorithm, we can deduce the following:

– The values for both clusters 3 and 4 remain fairly constant in each run which indicates artifacts with the same size appearing consistently in all frames. On the other hand, the values for cluster 2 behave more erratically and go up and down. This is due to appearing and disappearing of the artifact in some frames. Therefore, the detection is divided in multiple clusters along the time axis.
– Only cluster 1, the wear region, has values that consistently increase over time. This is in line with our expectation about an "ideal" wear that keeps growing. In practice, the wear may not expand over multiple acquisitions which will show itself as a plateau. However, it will never shrink or disappear so the values should remain

increasing overall. Moreover, even if the wear region becomes the most meaningful cluster only at frame 16, we can notice that it is the only growing cluster already at frames 11-12, meaning that we can trigger a "possible alteration" alert at this early stage.

The same deductions for WS01 can be observed for SV01, as well. This time we have three main clusters (see Fig. 6, right): cluster 1, the wear, and clusters 2 and 3, which are reflections present on most of the samples. In this case the alteration is correctly detected early than in sequence WS01. In fact, at frames 7-8, cluster 1 is both the most meaningful cluster and the most rapidly growing. This is coherent with the type of input data. Sequence WS01 displays the growing of a completely new damaged area, which is initially small and slowly growing, while SVO1 shows the worsening of an already worn-out region, thus it is reasonable that the new alteration appears earlier and grows faster.

Overall, results clearly show that, with respect to previous works leveraging single change maps [37], this analysis based on the temporal dynamics of the changes is able to pinpoint at an earlier stage and more reliably the emergence of a wear, in full accord with the preventive conservation principle.

5 Conclusions

In this paper, we introduced a probabilistic method for detecting significant changes located in clusters within a noisy multi-temporal series of images. The proposed method can be used in preventive conservation, as a fast preliminary examination of a varnished wooden surface able to identify the most likely new altered areas. Thus, a verification using more precise but slower techniques (like spectroscopic analyses) will be done only on these detected areas, optimizing the monitoring procedure. This approach, rooted in the Gestalt theory, is particularly interesting for the task of historical violin analysis with respect to other statistical learning-based and deep learning methods, given the limited amount of available data and also the difficulty of performing reliable annotations.

Future works will involve more tests, to further validate our approach, as well as refinements in the clustering method to achieve an even earlier detection of wear (ideally, as close as possible to the beginning of the alteration, when only a few pixels change).

Acknowledgments

References

1. Abas, F.S., Martinez, K.: Classification of painting cracks for content-based analysis. In: Proc. SPIE 5011, Machine Vision Applications in Industrial Inspection XI. vol. 5011, pp. 149–161 (2003)

2. Akinlar, C., Topal, C.: Edlines: A real-time line segment detector with a false detection control. Pattern Recognition Letters **32**(13), 1633 – 1642 (2011). https://doi.org/10.1016/j.patrec.2011.06.001

3. Aldea, E., Le Hégarat-Mascle, S.: Robust crack detection for unmanned aerial vehicles inspection in an a-contrario decision framework. Journal of Electronic Imaging **24**(6), 061119–061119 (2015)

4. Bradley, S.: Preventive conservation research and practice at the British museum. Journal of the American Institute for Conservation **44**(3), 159–173 (2005). https://doi.org/10.1179/019713605806082248

5. Cerimele, M.M., Cossu, R.: Decay regions segmentation from color images of ancient monuments using fast marching method. Journal of Cultural Heritage **8**(2), 170 – 175 (2007). https://doi.org/10.1016/j.culher.2007.01.006

6. Cerra, D., Plank, S., Lysandrou, V., Tian, J.: Cultural heritage sites in danger—towards automatic damage detection from space. Remote Sensing **8**(9), 781 (Sep 2016). https://doi.org/10.3390/rs8090781

7. Cornelis, B., Ruzic, T., Gezels, E., Dooms, A., Pizurica, A., Platisa, L., Cornelis, J., Martens, M., De Mey, M., Daubechies, I.: Crack detection and inpainting for virtual restoration of paintings: The case of the Ghent altarpiece. Signal Processing **93**(3), 605 – 619 (2013)

8. Deborah, H., Richard, N., Hardeberg, J.Y.: Hyperspectral crack detection in paintings. In: 2015 Colour and Visual Computing Symposium (CVCS). pp. 1–6 (2015). https://doi.org/10.1109/CVCS.2015.7274902

9. Desolneux, A., Moisan, L., Morel, J.M.: A grouping principle and four applications. IEEE Transactions on Pattern Analysis and Machine Intelligence **25**(4), 508–513 (2003)

10. Desolneux, A., Moisan, L., Morel, J.M.: Meaningful alignments. International journal of computer vision **40**(1), 7–23 (2000)

11. Desolneux, A., Moisan, L., Morel, J.M.: From gestalt theory to image analysis: a probabilistic approach, vol. 34. Springer Science & Business Media (2007)

12. Dondi, P., Lombardi, L., Invernizzi, C., Rovetta, T., Malagodi, M., Licchelli, M.: Automatic analysis of UV-induced fluorescence imagery of historical violins. Journal on Computing and Cultural Heritage **10**(2), 12:1–12:13 (2017). https://doi.org/10.1145/3051472

13. Dondi, P., Lombardi, L., Malagodi, M., Licchelli, M.: Automatic identification of varnish wear on historical instruments: The case of Antonio Stradivari violins. Journal of Cultural Heritage **22**, 968–973 (2016)

14. Dondi, P., Lombardi, L., Malagodi, M., Licchelli, M.: Segmentation of multi-temporal UV-induced fluorescence images of historical violins. In: New Trends in Image Analysis and Processing – ICIAP 2019. Lecture Notes in Computer Science, vol. 11808, pp. 81–91. Springer International Publishing (2019)

15. Fichera, G.V., Albano, M., Fiocco, G., Invernizzi, C., Licchelli, M., Malagodi, M., Rovetta, T.: Innovative monitoring plan for the preventive conservation of historical musical instruments. Studies in Conservation **63**(sup1), 351–354 (2018). https://doi.org/10.1080/00393630.2018.1499853

16. Fiorucci, M., Khoroshiltseva, M., Pontil, M., Traviglia, A., Del Bue, A., James, S.: Machine learning for cultural heritage: A survey. Pattern Recognition Letters **133**, 102–108 (2020). https://doi.org/https://doi.org/10.1016/j.patrec.2020.02.017

17. Flenner, A., Hewer, G.: A helmholtz principle approach to parameter free change detection and coherent motion using exchangeable random variables. SIAM Journal on Imaging Sciences **4**(1), 243–276 (2011)

18. Gelli, D., March, R., Salonia, P., Vitulano, D.: Surface analysis of stone materials integrating spatial data and computer vision techniques. Journal of Cultural Heritage **4**(2), 117 – 125 (2003)

19. Ghedini, N., Ozga, I., Bonazza, A., Dilillo, M., Cachier, H., Sabbioni, C.: Atmospheric aerosol monitoring as a strategy for the preventive conservation of urban monumental heritage: The florence baptistery. Atmospheric Environment **45**(33), 5979 – 5987 (2011). https://doi.org/10.1016/j.atmosenv.2011.08.001

20. Grosjean, B., Moisan, L.: A-contrario detectability of spots in textured backgrounds. Journal of Mathematical Imaging and Vision **33**(3), 313 (2009)

21. Guarneri, M., Danielis, A., Francucci, M., Collibus, M.F.D., Fornetti, G., Mencattini, A.: 3D remote colorimetry and watershed segmentation techniques for fresco and artwork decay monitoring and preservation. Journal of Archaeological Science **46**, 182 – 190 (2014)

22. Invernizzi, C., Fichera, G.V., Licchelli, M., Malagodi, M.: A non-invasive stratigraphic study by reflection FT-IR spectroscopy and UV-induced fluorescence technique: The case of historical violins. Microchemical Journal **138**, 273 – 281 (2018). https://doi.org/10.1016/j.microc.2018.01.021

23. Janssens, K., Van Grieken, R.: Non-destructive micro analysis of cultural heritage materials, vol. 42. Elsevier (2004)

24. Khelifi, L., Mignotte, M.: Deep learning for change detection in remote sensing images: Comprehensive review and meta-analysis. IEEE Access **8**, 126385–126400 (2020)

25. Li, M.D., Chang, K., Bearce, B., Chang, C.Y., Huang, A.J., Campbell, J.P., Brown, J.M., Singh, P., Hoebel, K.V., Erdoğmuş, D., et al.: Siamese neural networks for continuous disease severity evaluation and change detection in medical imaging. NPJ digital medicine **3**(1), 1–9 (2020)

26. Lisani, J.L., Morel, J.M.: Detection of major changes in satellite images. In: Proceedings 2003 International Conference on Image Processing (Cat. No. 03CH37429). vol. 1, pp. I–941. IEEE (2003)

27. Liu, G., Gousseau, Y., Tupin, F.: A contrario comparison of local descriptors for change detection in very high spatial resolution satellite images of urban areas. IEEE Transactions on Geoscience and Remote Sensing (2019)

28. Lucchi, E.: Review of preventive conservation in museum buildings. Journal of Cultural Heritage **29**, 180 – 193 (2018). https://doi.org/10.1016/j.culher.2017.09.003

29. Mandal, M., Vipparthi, S.K.: An empirical review of deep learning frameworks for change detection: Model design, experimental frameworks, challenges and research needs. IEEE Transactions on Intelligent Transportation Systems (2021)

30. Manferdini, A.M., Baroncini, V., Corsi, C.: An integrated and automated segmentation approach to deteriorated regions recognition on 3D reality-based models of cultural heritage artifacts. Journal of Cultural Heritage **13**(4), 371 – 378 (2012). https://doi.org/10.1016/j.culher.2012.01.014

31. Michaelsen, E.: Self-organizing maps and gestalt organization as components of an advanced system for remotely sensed data: An example with thermal hyper-spectra. Pattern Recognition Letters **83**, 169 – 177 (2016). https://doi.org/10.1016/j.patrec.2016.06.004, advances in Pattern Recognition in Remote Sensing

32. Moulon, P., Monasse, P., Marlet, R.: Adaptive structure from motion with a contrario model estimation. In: Asian Conference on Computer Vision. pp. 257–270. Springer (2012)

33. Ortiz, R., Ortiz, P.: Vulnerability index: A new approach for preventive conservation of monuments. International Journal of Architectural Heritage **10**(8), 1078–1100 (2016). https://doi.org/10.1080/15583058.2016.1186758

34. Perles, A., Pérez-Marín, E., Mercado, R., Segrelles, J.D., Blanquer, I., Zarzo, M., Garcia-Diego, F.J.: An energy-efficient internet of things (IoT) architecture for preventive conservation of cultural heritage. Future Generation Computer Systems **81**, 566 – 581 (2018). https://doi.org/10.1016/j.future.2017.06.030

35. Pizurica, A., Platisa, L., Ruzic, T., Cornelis, B., Dooms, A., Martens, M., Dubois, H., Devolder, B., De Mey, M., Daubechies, I.: Digital image processing of the ghent altarpiece: Supporting the painting's study and conservation treatment. IEEE Signal Processing Magazine **32**(4), 112–122 (2015). https://doi.org/10.1109/MSP.2015.2411753

36. Rezaei, A., Aldea, E., Dondi, P., Malagodi, M., Le Hégarat-Mascle, S.: Detecting alterations in historical violins with optical monitoring. In: Proceedings of the 14th International Conference on Quality Control by Artificial Vision (QCAV). vol. 11172, pp. 1117210–1 – 1117210–8 (2019). https://doi.org/10.1117/12.2521702

37. Rezaei, A., Le Hégarat-Mascle, S., Aldea, E., Dondi, P., Malagodi, M.: One step clustering based on a-contrario framework for detection of alterations in historical violins. In: 25th International Conference on Pattern Recognition (ICPR2020). p. 9348 – 9355 (2021)

38. Robin, A., Moisan, L., Le Hégarat-Mascle, S.: An a-contrario approach for subpixel change detection in satellite imagery. IEEE Transactions on Pattern Analysis and Machine Intelligence **32**(11), 1977–1993 (2010)

39. Rousseau, F., Faisan, S., Heitz, F., Armspach, J.P., Chevalier, Y., Blanc, F., de Seze, J., Rumbach, L.: An a contrario approach for change detection in 3D multimodal images: application to multiple sclerosis in mri. In: 2007 29th Annual International Conference of the IEEE Engineering in Medicine and Biology Society. pp. 2069–2072. IEEE (2007)

40. Rovetta, T., Invernizzi, C., Fiocco, G., Albano, M., Licchelli, M., Gulmini, M., Alf, G., Rombolà, A., Malagodi, M.: The case of Antonio Stradivari 1718 ex-San Lorenzo violin: History, restorations and conservation perspectives. Journal of Archaeological Science: Reports **23**, 443–450 (2019). https://doi.org/10.1016/j.jasrep.2018.11.010

41. Rovetta, T., Invernizzi, C., Licchelli, M., Cacciatori, F., Malagodi, M.: The elemental composition of Stradivari's musical instruments: new results through non-invasive EDXRF analysis. X-Ray Spectrometry **47**(2), 159–170 (2018). https://doi.org/10.1002/xrs.2825

42. Sturari, M., Paolanti, M., Frontoni, E., Mancini, A., Zingaretti, P.: Robotic platform for deep change detection for rail safety and security. In: 2017 European Conference on Mobile Robots (ECMR). pp. 1–6. IEEE (2017)

43. Varghese, A., Gubbi, J., Ramaswamy, A., Balamuralidhar, P.: Changenet: A deep learning architecture for visual change detection. In: Proceedings of the European Conference on Computer Vision (ECCV) Workshops. pp. 0–0 (2018)

44. Veit, T., Cao, F., Bouthemy, P.: An a contrario decision framework for region-based motion detection. International journal of computer vision **68**(2), 163–178 (2006)

45. Veit, T., Cao, F., Bouthemy, P.: Space-time a contrario clustering for detecting coherent motions. In: Proceedings 2007 IEEE International Conference on Robotics and Automation. pp. 33–39. IEEE (2007)

46. Verma, S., Panigrahi, A., Gupta, S.: Qfabric: Multi-task change detection dataset. In: Proceedings of the IEEE/CVF Conference on Computer Vision and Pattern Recognition. pp. 1052–1061 (2021)

47. Widynski, N., Mignotte, M.: A contrario edge detection with edgelets. In: 2011 IEEE International Conference on Signal and Image Processing Applications (ICSIPA). pp. 421–426. IEEE (2011)

48. Yan, Y., Ren, J., Sun, G., Zhao, H., Han, J., Li, X., Marshall, S., Zhan, J.: Unsupervised image saliency detection with gestalt-laws guided optimization and visual attention based refinement. Pattern Recognition **79**, 65 – 78 (2018). https://doi.org/10.1016/j.patcog.2018.02.004